

Chapter 5 The Rate Form of the Equation of State

5.1 Introduction

5.1.1 Chapter Overview

In conjunction with the usual rate forms of the conservation equations, the time derivative form of the Equation of State is investigated from a numerical consideration point of view. By recasting the equation of state in a form that is on equal footing with the system conservation equations, several advantages are found. The rate method is found to be more intuitive for system analysis, more appropriate for eigenvalues extraction, as well as easier to program and to implement. Numerically, the rate method is found [GAR87a] to be more efficient and as accurate than the traditional iterative method.

5.1.2 Learning Outcomes

Objective 5.1	The student should be able to develop a flow diagram and pseudo-code for the rate method of the equation of state.					
Condition	Open book written examination.					
Standard	100%.					
Related concept(s)	The rate form of the equation of state.					
Classification	Knowledge	Comprehension	Application	Analysis	Synthesis	Evaluation
Weight	a	a	a			

Objective 5.2	The student should be able to develop a computer code implementing the rate method of the equation of state.					
Condition	Workshop or project based investigation.					
Standard	100%. Any computer language may be used.					
Related concept(s)	The rate form of the equation of state.					
Classification	Knowledge	Comprehension	Application	Analysis	Synthesis	Evaluation
Weight	a	a	a			

Objective 5.3	The student should be able to model a simple thermalhydraulic network using the integral form of the conservation equations and the rate form of the equation of state. The student should be able to check for reasonableness of the answers.					
Condition	Workshop or project based investigation.					
Standard	100%.					
Related concept(s)	Integral form of the conservation equations. Node-link diagram. The rate form of the equation of state.					
Classification	Knowledge	Comprehension	Application	Analysis	Synthesis	Evaluation
Weight	a	a	a	a		

5.1.3 Chapter Layout

First, the derivation of the rate form of the Equation of State is presented. Systematic comparison between the new method and the traditional iterative method is made by applying the methods to a simple flow problem. The comparison is then extended to a practical engineering problem requiring accurate prediction of pressure.

5.2 The Rate Form

Presently, the conservation equations are all cast as rate equations whereas the equation of state is typically written as an algebraic equation [AGE83]. This arises from the basic assumption that, although the properties of mass, momentum and energy must be traced or solved as a function of time and space, the corresponding local pressure is a pure function of the local state of the fluid. Hence the equation of state is considered only as a constitutive equation. This treatment puts the pressure determinations on the same level as heat transfer coefficients. Although numerical solution of the resulting equation sets give correct answers (to within the accuracy of the assumption), intuition is not generated and time-consuming iterations must be performed to get a pressure consistent with the local state parameters.

The time derivative form of the Equation of State is investigated, herein, in conjunction with the usual rate forms of the conservation equations. This gives an equation set with two distinct advantages over the use of algebraic form of the Equation of State normally used.

The first advantage is that the equation set used consists of four equations for each node or point in space, characterizing the four main actors: mass, flow, energy and pressure. This consistent formulation permits the straight-forward extraction of the system eigenvalues (or characteristics) without having to solve the equations numerically. Theoretical analysis of this aspect is given in appendix 5.

The second advantage is that the rate form of the Equation of State permits the numerical calculation of the pressure without iteration. The calculation time for the pressure was found to be reduced by a factor of more than 20 in some cases (where the flow was rapidly varying) and, at worst, the rate form was no slower than the algebraic form. In addition, because the pressure can be explicitly expressed in terms of slowly varying system parameters and flow, an implicit numeric scheme is easily formulated and coded.

This chapter will concentrate on this numerical aspect of the equation of state.

The equation of state has been discussed in chapter 4 where we saw that the determination of pressure from known values of other thermodynamic properties is not direct. Interpolation and iteration is required because the independent (known) parameters are temperature, T, and pressure, P. Unfortunately, T and P are rarely the independent parameters in system dynamics since the numerical solution of the conservation equations yield mass and energy as a function of time. Hence, from the point of view of the equation of state, it is mass and energy which are the independent parameters. Consequently, system codes are hampered by the form of water property data.

Having derived the desired rate forms for the equation of state in chapter 4, we proceed to illustrate the utility of the approach.

5.3 Numerical Investigations: a Simple Case

The simple two-node, one-link system is (Figure 5.1) chosen to illustrate the effectiveness of the rate form of the equation of state in eliminating the inner iteration loop in thermalhydraulic simulations. In general, the task is to solve the matrix equation,

$$\frac{\partial \mathbf{u}}{\partial t} = \mathbf{A}\mathbf{u} + \mathbf{b} \quad (1)$$

over the time domain of interest. The key point that we wish to discuss is the difference in the normal method (where $\mathbf{u} = \{M_1, H_1, W, M_2, H_2\}$) and the rate method (where $\mathbf{u} = \{M_1, H_1, P_1, W, M_2, H_2, P_2\}$). For simplicity and clarity, we first summarize work for a fixed time step Euler integration:

$$\mathbf{u}^{t+\Delta t} = \mathbf{u}^t + \Delta t[\mathbf{A}\mathbf{u} + \mathbf{b}] \quad (2)$$

As we shall see, this is sufficient to generate some observations on the utility of the rate method. These observations then guide us in the use of more complicated and efficient algorithms.

5.3.1 Normal Method

The normal method obtains the value of pressure at time, $t+\Delta t$, from an iteration (as discussed previously) on the equation of state using the values of mass and enthalpy at time, $t+\Delta t$, i.e. the new pressure must satisfy:

$$P^{t+\Delta t} = \text{fn}(\rho^{t+\Delta t}, h^{t+\Delta t}) \quad (3)$$

where both ρ and h are pressure dependent functions. Any iteration requires a starting guess and a feedback mechanism. Here, the starting guess for pressure is the value at time, t : P^t . Feedback in the Newton-Raphson scheme is generated by using an older value of pressure, $P^{t-\Delta t}$, to estimate slopes. Since the slope, $\partial h/\partial P$, was readily available from the rate method, we chose to use this slope to guide feedback. Thus, in the comparison of methods, we have borrowed from the rate method to enhance the normal method. This provides a stronger test of the rate method.

Thus we can now generate our next pressure guess from:

$$P_{\text{new}} = P_{\text{guess}} + \frac{h - h_{\text{est}}}{\partial h/\partial P} * \text{ADJ} \quad (4)$$

where h is the known value of h at $t+\Delta t$ and h_{est} is the estimated h based on the guessed pressure as discussed in detail in chapter 4. ADJ is an adjustment factor $\in [0, 1]$, to allow experimentation with the amount of feedback. This iteration on pressure continues until a convergence criteria, P_{err} , is satisfied. The converged pressure is used in the outer loop in the momentum equation and the time can be advanced one time step. Figure 5.2 summarizes the logic flow.

5.3.2 Rate Method

The rate method obtains the value of pressure at time, $t+\Delta t$, directly from the rate equation as is done for the conservation equations. Equation 27 of chapter 4, gives the rate of change of pressure which can be solved simultaneously with the conservation equations if substitutions for dM/dt and dH/dt are made, leading to:

$$\frac{\partial \mathbf{u}}{\partial t} = \mathbf{A}\mathbf{u} + \mathbf{b} \quad (5)$$

where $\mathbf{u} = \{M_1, H_1, P_1, W, M_2, H_2, P_2\}$.

Thus:

$$\mathbf{P}_i^{t+\Delta t} = \mathbf{P}_i^t + \Delta t[\mathbf{A}\mathbf{u} + \mathbf{b}]_i \quad (6)$$

No inner iteration is required, as shown in Figure 5.3.

One problem with this approach is that the pressure may drift away from a value consistent with the mass and energy. This problem does not arise with the conservation equations because the equations are conservative in form, by design. It is not possible to cast the rate form of the equation of state in conservative form since pressure is simply not a conserved property. We can surmount the drift problem by using the feedback philosophy of the normal method. Thus the new pressure is given by:

$$\mathbf{P}_i^{t+\Delta t} = \mathbf{P}_i^t + \Delta t[\mathbf{A}\mathbf{u} + \mathbf{b}]_i + \frac{h-h_{est}}{\partial h/\partial P} * ADJ \quad (7)$$

This correction term uses only readily available information in a non-iterative manner.

In essence, the main effective difference between the normal and rate method is that during the time step between t and $t+\Delta t$ the normal method employs parameters such as density, quality etc. derived from the pressure at time, $t+\Delta t$, whereas the rate form employs parameters derived from the pressure and rate of change of pressure at time, t . The normal method is not necessarily more accurate, it is simply forcibly implicit in its treatment of pressure. The rate method can be implicit (as we shall see) but it need not be. Without experimentation it is not evident whether the necessity of iteration in the normal method is outweighed by the possible advantages of the implicit pressure treatment.

The next sections tests these issues with numerical experiments.

5.3.3 Comparison

The two node, one link numerical case under consideration is summarized in figure 5.1. Perhaps the most startling difference between the normal and rate methods is the difference in programming effort. The rate form was found to be extremely easy to implement since the equation form is the same as the continuity equations. The normal method took roughly twice the time to implement since separate control

of the pressure logic is required. This arises directly from the treatment of pressure in the normal method: it is the odd man out.

The second startling difference was ease of execution of the rate form compared to the normal form. The normal form required experimentation with both the pressure convergence tolerance, P_{err} , and the adjustment factor, ADJ, since the solution was sensitive to both parameters. The rate method contains only the adjustment factor ADJ. The first few runs of the rate method showed that since the correction term for drift $(h-h_{est})/(\partial h/\partial p)$ is always several orders of magnitude below the primary update term, $\Delta t\{\mathbf{A}\mathbf{u} + \mathbf{b}\}$, the solution was not at all sensitive to the value of ADJ. Thus the rate method proved easier to program and easier to run than the normal method.

We look at the number of iterations required for pressure convergence as a function of P_{err} and ADJ for the normal method without regard to accuracy. For a Δt of 0.01sec, $P_{err} = 10^{-3}$ (fraction of the full scale pressure of 10 MPa), the effect of ADJ is seen in figure 5.4. This result is typical: an adjustment factor of 1 gives rapid convergence (one or two iterations) except where very large pressure changes occur. For the case of very rapid changes, the full feedback (ADJ = 1) causes overshoot. Overall, however, the time spent for pressure calculation is about the same, independent of ADJ.

Allowing a larger pressure error had the expected result of reducing the number of iterations needed per routine call. But choosing a smaller time step (say .001) did not have a drastic effect on the peak iterations required. The rate method, of course, always used 1 iteration per routine call and the adjustment factor ADJ was found to be unimportant since the drift correction factor amounted to no more than 1% of the total pressure update term.

The integrated error for both methods is shown in figure 5.5. Both methods converge rapidly to the benchmark. The value of P_{err} is not overcritical. A value of P_{err} consistent with tolerances set for other simulation variables is recommended. The time spent per each iteration is roughly comparable for both methods. The main difference is that the rate method requires the evaluation of the F functions over and above the property calls common to both methods. This minor penalty is insignificant in all cases studied since the number of iterations / call dominated the calculation time.

In summary, to this point, the rate method is easier to implement, more robust and is equal to the normal method at worst, more than 20 times faster under certain conditions. We now look at incorporating a variable time step to see how each method compares.

Typical variable time step algorithms require some measure of the rate of change of the main variables to guide the Δt choice. The matrix equation, equation 1, provides the rates that we need. Since the rate method incorporated the pressure into the \mathbf{u} vector, the rate of change of pressure is immediately available. For the normal method, the rate of change of pressure has to be estimated from previous history (which is no good for predicting the onset of rapid changes) or by trial and error. The trial and error method employed here is to calculate the Δt as the minimum of the time steps calculated from:

$$\Delta t_i = \frac{(\text{fractional tolerance}) \times (\text{scale factor for } u_i)}{\partial u_i / \partial t} \quad (8)$$

This restricts Δt so that no parameter changes more than the prescribed fraction for that parameter. This can be implemented in a non-iterative manner for the rate method. However, for the normal method, the above minimum Δt based on \mathbf{u} is used as the test Δt for the pressure routine and the rate of change of

pressure is estimated as:

$$\frac{\partial P}{\partial t} = \frac{P^{t+\Delta t} - P^t}{\Delta t} \quad (9)$$

The Δt is then scaled down if the pressure change is too large for that iteration. Then the new Δt is tested to ensure that it indeed satisfies the pressure change limit. This iteration loop has within it the old inner loop.

It is expected then, that the normal method will not perform as well as the rate method primarily because of the "loop within a loop" inherent in the normal method as applied to typical system simulation codes.

A number of cases were studied and the results of the normal method were compared to the rate method. The figure of merit was chosen as

$$\text{F.O.M.} = \frac{10,000}{(\text{integrated error}) \times (\text{total pressure routine time}) \times (\text{No. of adjustable parameters})} \quad (10)$$

Thus, an accurate, fast and robust method achieves a high figure of merit. Some results are listed in table 5.1. Derating a method with more adjustable parameters is deemed appropriate because of the figure of merit should reflect the effort involved in using that method. On average, about 6 runs of the normal method, with various P_{err} and ADJ were needed to scope out the solution field compared to 1 run for the rate method. Thus a derating of 2 is not an inappropriate measure of robustness or effort required.

The results indicate that the rate method is a consistently better method than the normal method in terms of numerical performance. We see no reason why this improvement would not exist for any thermal hydraulic system in which pressure field determination is required.

Next we briefly discuss implicit numerical schemes.

The nodal equations are:

$$\frac{dM_1}{dt} = -W \quad \text{and} \quad \frac{dM_2}{dt} = +W \quad (11)$$

$$\frac{dH_1}{dt} = -h_1 W \quad \text{and} \quad \frac{dH_2}{dt} = +h_1 W \quad (12)$$

$$\frac{dP_i}{dt} = \frac{F_1 \frac{dM_1}{dt} + F_2 \frac{dH_i}{dt}}{M_g F_4 + M_f F_5}, \quad i = 1, 2 \quad (13)$$

Considering just the flow and pressure rate equations, we have (after substituting in for dM/dt and dH/dt):

$$\frac{dW}{dt} = \frac{A}{L}(P_1 - P_2) - \frac{A}{L}K|W|W \quad (14)$$

and

$$\frac{dP_1}{dt} = -\chi_1 W \quad \text{and} \quad \frac{dP_2}{dt} = +\chi_2 W \quad (15)$$

where χ_1 and χ_2 are > 0 and are given by:

$$\chi = \frac{F_1 + hF_2}{M_g F_4 + M_f F_5} \quad (16)$$

evaluated at the local property values of nodes 1 and 2.

Employing a scheme that is implicit in flow, the difference equations are cast

$$\frac{W^{t+\Delta t} - W^t}{\Delta t} = \frac{A}{L}(P_1^{t+\Delta t} - P_2^{t+\Delta t}) - \frac{A}{L}K|W^t|W^{t+\Delta t} \quad (17)$$

$$\frac{P_i^{t+\Delta t} - P_i^t}{\Delta t} = \pm\chi_i W^{t+\Delta t} \Rightarrow P_i^{t+\Delta t} - P_i^t = \pm\chi_i W^{t+\Delta t} \Delta t \quad (18)$$

Collecting terms and solving for the new flow:

$$W^{t+\Delta t} = \left[1 + \frac{A}{L}K|W^t|\Delta t + \frac{A}{L}(\chi_1 + \chi_2)\Delta t^2 \right]^{-1} \left[W^t + \frac{A}{L}(P_1^t - P_2^t)\Delta t \right] \quad (19)$$

This is the implicit time advancement algorithm employing the rate form of the equation of state. For the normal method, the pressure rate equation in terms of flow (i.e., equation 18) is not available to allow an implicit formulation of the pressure. Consequently, the implicit time advancement algorithm for the normal method is:

$$W^{t+\Delta t} = \left[1 + \frac{A}{L}K|W^t|\Delta t \right]^{-1} \left[W^t + \frac{A}{L}(P_1^{t+\Delta t} - P_2^{t+\Delta t})\Delta t \right] \quad (20)$$

To appreciate the difference between equations 19 and 20, consider the eigenvalues and vectors of

$$\frac{\partial \mathbf{u}(t)}{\partial t} = \mathbf{A}(\mathbf{u}, t)\mathbf{u}(t) \quad (21)$$

If we assume, over the time step under consideration, that $\mathbf{A} = \text{constant}$ and has distinct eigenvalues, then the solution to equation 21 can be written as:

$$\mathbf{u}(t) = \sum_{\ell=1}^N \mathbf{u}_\ell e^{\alpha_\ell t} \quad (22)$$

where $\mathbf{u}_\ell = \text{eigenvectors}$
 $\alpha_\ell = \text{eigenvalues.}$

It can be shown that for the explicit formalism, the numerical solution is equivalent to:

$$\mathbf{u}^{t+\Delta t} = \sum_{\ell=1}^N (1 + \alpha_\ell \Delta t) \mathbf{u}_\ell \quad (23)$$

while the implicit form is:

$$\mathbf{u}^{t+\Delta t} = \sum_{\ell=1}^N \frac{\mathbf{u}_\ell}{(1 - \alpha_\ell \Delta t)} \quad (24)$$

The eigenvalues can often be large and negative. Thus, at some Δt , the factor $(1+\alpha_i\Delta t)$ can go negative in the explicit solution causing each subsequent evaluation of \mathbf{u} to oscillate in sign and go unstable. For the implicit method, the contributions due to large negative eigenvalues decays away as $\Delta t \rightarrow \infty$. Thus the implicit formalism tend to be very well behaved at large time steps. Positive eigenvalues, by a similar argument pose a threat to the implicit form. However, this is not a practical problem because $\alpha_i\Delta t$ is kept $\ll 1$ for accuracy reasons. Thus, as long as the solution algorithm contains a check on the rate of growth or decay (effectively the dominant eigenvalues) then the implicit form is well behaved.

With this digression in mind, we see that the implicit rate formalism (equation 19) has more of the system behaviour represented implicitly than the normal method (equation 20). Thus, we might expect the rate form to be more stable than the normal form. Indeed, this was found to be the case as shown in figure 5.6. For a fixed and large time step (0.1sec.) the normal method showed the classic numerical instability due to the explicit pressure treatment. The rate form is well damped and very stable, showing that this method should permit the user to "calculate through" pressure spikes if they are not of interest.

5.4 Numerical Investigations: a Practical Case

The comparison between the normal and rate methods is extended to a practical application where a two node homogeneous model is used to simulate a transient of a small pressurizer operating at near-atmospheric pressure. The procedure is briefly described in the following [SOL85].

Figure 5.7 illustrates the problem. Steam and stratified liquid water in the pressurizer are schematically shown as two control volumes (nodes). The nodal fluids are assumed to be at saturated two-phase conditions corresponding to the pressure at their respective control volumes. The overall boundary conditions to the system are the steam bleed flow at the top of the pressurizer, the flow into and out of the pressurizer through the surge line, heat input from heaters at the bottom of the pressurizer and heat loss to pressurizer wall.

The rate of change of mass, M_S in the steam control volume and M_L in the liquid control volume, can be expressed by the following:

$$\frac{dM_S}{dt} = -W_{STB} - W_{CD} - W_{CI} + W_{EI} + W_{BR} \quad (25)$$

$$\frac{dM_L}{dt} = W_{SRL} - W_{EI} - W_{BR} + W_{CD} + W_{CI} \quad (26)$$

where W_{STB} is the steam bleed flow, W_{SRL} is the surge line inflow, W_{CI} is the interface condensation rate at the liquid surface separating the steam control volume from the liquid control volume, W_{EI} is the interface evaporation rate at the same liquid surface, W_{CD} is the flow of condensate droplets (liquid phase) from the bulk of the steam control volume toward the liquid control volume, and W_{BR} is the rising flow of bubbles (gas phase) from the bulk of liquid volume toward the steam volume.

The rate of change of energy in the two control volumes can be expressed by the rate of change in the total enthalpy, H_S and H_L , in the steam and liquid control volumes respectively:

$$\frac{dH_S}{dt} = -W_{STB}h_{gST} - W_{CD}h_{fST} - W_{CI}h_{gST} + W_{EI}h_{sLQ} + W_{BR}h_{gLQ} - Q_{WS} + Q_{TR} - (1-\beta)[(1-\delta)Q_{COND} + Q_{EVPR}] \quad (27)$$

and

$$\frac{dH_L}{dt} = W_{SRL}h_{SRL} - W_{EI}h_{fLQ} - W_{BR}h_{gLQ} + W_{CI}h_{fST} + W_{CD}h_{fST} - Q_{WL} + Q_{PWR} - Q_{TR} - \beta[(1-\delta)Q_{COND} + Q_{EVPR}] \quad (28)$$

where h_{SRL} is the specific enthalpy of the fluid in the surge line, h_{gST} and h_{fST} are respectively the saturated gas phase specific enthalpy and the saturated liquid phase specific enthalpy in the steam control volume, h_{gLQ} and h_{fLQ} are respectively the saturated gas phase specific enthalpy and the saturated liquid phase specific enthalpy in the liquid control volume, Q_{WS} and Q_{WL} are the rate of heat loss to the wall in the steam control volume and in the liquid control volume respectively, Q_{TR} is the heat transfer rate from the liquid control volume to the steam control volume due to any temperature gradient, excluding those due to interface evaporation and condensation; Q_{COND} is the rate of energy released by the condensing steam to both the steam and liquid control volumes during the interface condensation process and Q_{EVPR} is rate of energy absorbed by the evaporating liquid from both the steam and liquid control volumes during the interface evaporation process. The constant, β , represents the fraction of these energies distributed to or contributed by the liquid control volume. The ratio δ represents the portion of energy released during the interface condensation that is lost to the wall.

The calculation of swelling and shrinking of control volumes is only done for the liquid control volume and the volume in the steam control volumes will be related to the volume in the liquid control volume, V_L , as:

$$\frac{dV_S}{dt} = -\frac{dV_L}{dt} \quad (29)$$

The swelling and shrinking of the liquid control volume as well as values of W_{STB} , W_{SRL} , W_{CI} , W_{EI} , W_{CD} , W_{BR} , Q_{WS} , Q_{WL} , Q_{TR} , Q_{PWR} , β and δ are calculated using analytical or empirical constitutive equations. The majority of these parameters depend directly or indirectly on pressure. Any inaccurate prediction of pressure during a numerical simulation will result in severe numerical instability. Hence the above problem is a good testing ground for comparing the performances of the two methods.

During the test simulation, the pressurizer is initially at a quasi-steady state. The steam pressure is at 96.3 kPa. The steam bleed flow, W_{STB} , heater power Q_{PWR} and heat losses Q_{WL} and Q_{WS} are at their quasi-steady values, maintaining the saturation condition of the pressurizer. At time = 11 sec., the steam bleed valve is closed and W_{STB} drops to zero while Q_{PWR} is increased to a fixed value of 300 Watts. At time = 16 sec., the steam bleed valve is reopened and its set point set at 80 kPa.

Since the thermodynamic properties in the steam control volume and the liquid control volume are functions of P_S and P_L (pressures of the respective control volumes), there are seven unknowns from equations 21 to 25, namely: M_S , M_L , H_S , H_L , V_S (or V_L), P_S and P_L . Adding two equations of state, one for each control volume, will complete the equation set:

$$P_S = \text{fn}(\rho_S, h_S) = \text{fn}\left(\frac{M_S}{V_S}, \frac{H_S}{M_S}\right) \quad (30)$$

$$P_L = \text{fn}(\rho_L, h_L) = \text{fn}\left(\frac{M_L}{V_L}, \frac{H_L}{M_L}\right) \quad (31)$$

Both the normal iterative method and the rate method are tested to solve Equations 26 and 27. The following observations are made:

- Using the normal method, the choice of adjusting P to converge on h given ρ or converging on ρ given h is found to be very important in providing a stable numerical result. At time step = 10 msec, no complete simulation result can be generated when ρ was the adjusted variable. An explanation of this can be given by referring to $G_1(P, x)$, or $\partial P / \partial \rho$. This factor is proportional to the square of $[x v_g(P) + (1-x)v_l(P)]$. However, the direction of change in the saturated gas phase specific volume with pressure is opposite to that of saturated liquid phase specific volume:

$$\begin{aligned} dv_g/dP &> 0 \\ dv_l/dP &< 0 \end{aligned}$$

Therefore, a fluctuation in the value of pressure during an iteration process will amplify the fluctuation in the value of predicted density when that method is used;

- Using enthalpy as the adjusted variable to converge on P , simulation results can be generated if an error tolerance E of less than 0.2% is used. The error tolerance is defined as:

$$E = \frac{\text{ABS}(h - h_{\text{estimate}})}{h} \times 100\%$$

Figure 5.8 shows the transient of P_L and P_S for $E = 0.2\%$. Unstable solutions result for E higher than 0.2%. The average number of iteration is found to depend on the error tolerance as shown in figure 5.10.

- On the other hand, the performance of the rate method is much more convincing in both accuracy and efficiency. The transient of P_L and P_S predicted using the rate method is shown in Figure 5.9.

5.5 Discussion And Conclusion

The rate form is a cogent expression of the equation of state that is distinct from the normal algebraic form. The essential difference is that the rate form expresses the relationship between the rates of change of the state variables, while the normal form relates the static values of the state variables. Although this is stating the obvious, the change in viewpoint is revealing.

No barrier is perceived to applying the rate form to the multi-node/link case, to the distributed form of the basic equations, and to eigenvalue extraction (numerical or analytical).

Although we have not made use of it in this work, the non-equilibrium form (equations 4.42 and 4.43) is provocative. It entices one to view the non-equilibrium situation as the essentially dynamic situation that it is and helps to focus our attention on the thermal relaxation. Given the temperature rate equations, the non-equilibrium situation should be easy to incorporate without a major code rewrite.

We conclude by restating our major findings. The rate method offers many advantages:

- It is more intuitive for system work. It permits a proper focus on the two main actors, flow and pressure.
- The same form is appropriate for eigenvalue extraction as well as numerical simulation. This extends the usefulness of coding.
- Programs are easier to implement.

- 4) Programs are more robust and require less hand holding.
- 5) Time step control and detection of rapid changes (like phase changes) is improved.

Overall the method is usually faster and more accurate. Time savings peaked at a ratio of 26 for the cases considered.

5.6 Exercises

1. Consider 2 connected volumes of water with conditions as shown in figure 5.1 Model this with 2 nodes and 1 link. Use the supplied code (2node.c) as a guide.
 - a. Solve for the pressure and flow histories using the normal iterative method for the equation of state,
 - b. Solve for the pressure and flow histories using the non-iterative rate method.
 - c. Compare the two solutions and comment.

2. Vary the initial conditions of question 1 so as to cause void collapse in volume 2 during the transient. What problems can you anticipate? Solve this case by both methods.

Table 5.1 Figure of Merit Comparisons of the Normal and Rate Forms of the Equation of State for Various Convergence Criteria (Simple Case).

Case	Method	Convergence (fraction full scale)		ADJ	Integral error	Pressure routine time	AP*	FOM*	Relative* FOM
		Overall	Pressure						
1	P rate	0.01		0.5	180.39	24	1	2.31	
2	P norm	0.01	0.01	0.5	597.61	25	2	0.33	6.90
3	P rate	0.001		0.5	21.13	96	1	4.93	
4	P norm	0.001	0.001	0.5	79.819	119	2	0.53	9.37
5	P norm	0.001	0.00001	1	22.808	246	2	0.89	5.53
6	P norm	0.001	0.0001	1	22.781	229	2	0.96	5.14
7	P norm	0.001	0.001	1	22.761	140	2	1.57	3.14
8	P norm	0.001	0.01	1	22.847	128	2	1.71	2.88
9	P rate	0.0001		0.5	0.534	736	1	25.44	
10	P norm	0.0001	0.0001	0.5	2.2536	852	2	2.60	9.77
11	P norm	0.0001	0.0001	1	0.4907	894	2	11.40	2.23

* AP = # of adjustable parameters

FOM = Figure of merit

Relative FOM = (FOM for rate method)/(FOM for normal method)

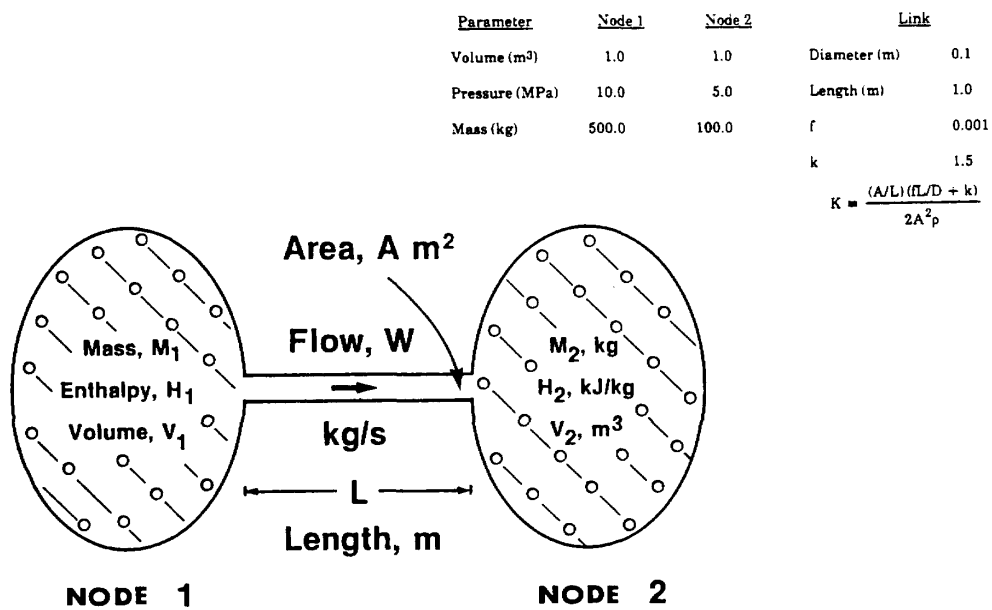


Figure 5.1 Simple 2-node, 1-link system.

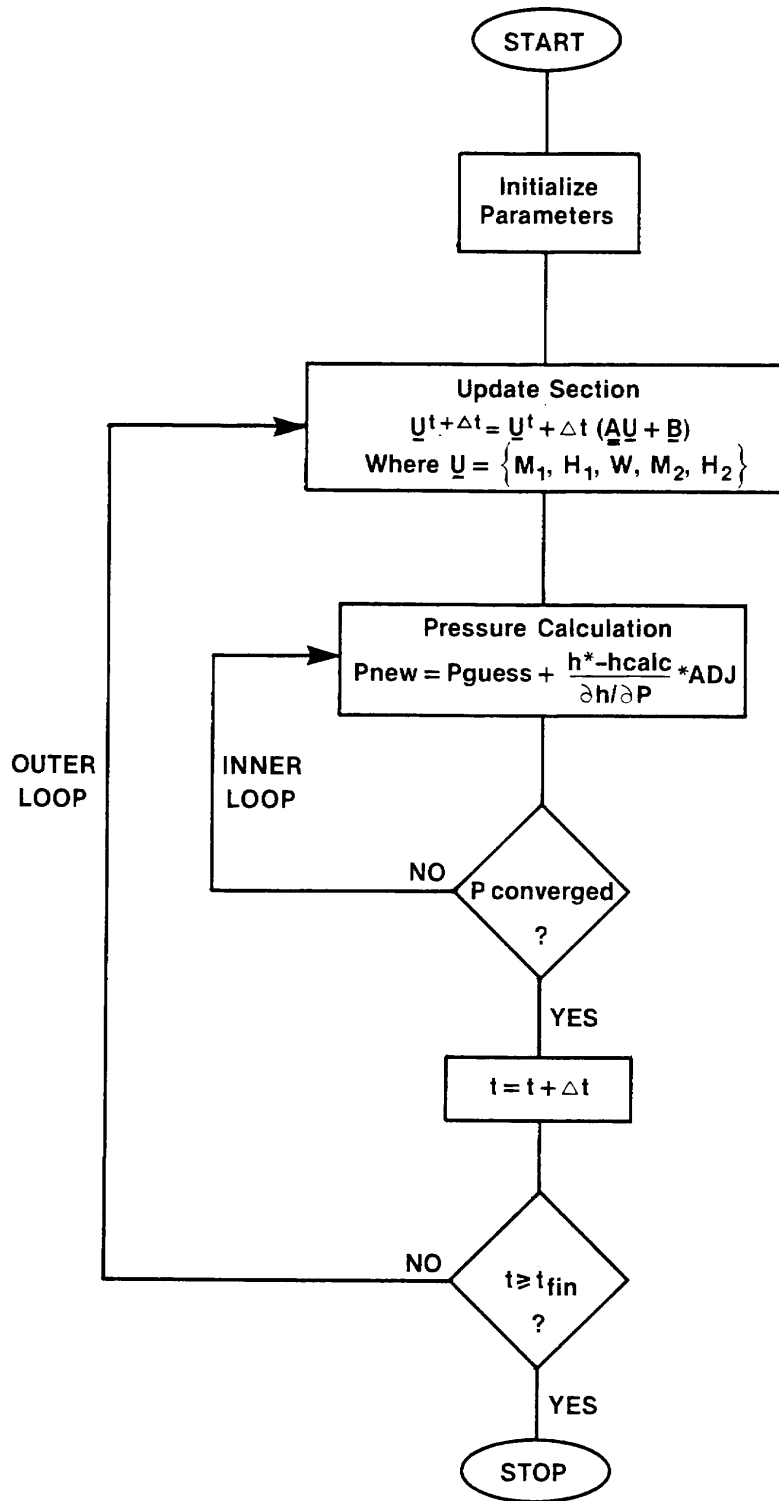


Figure 5.2 Program flow diagram for the normal method.

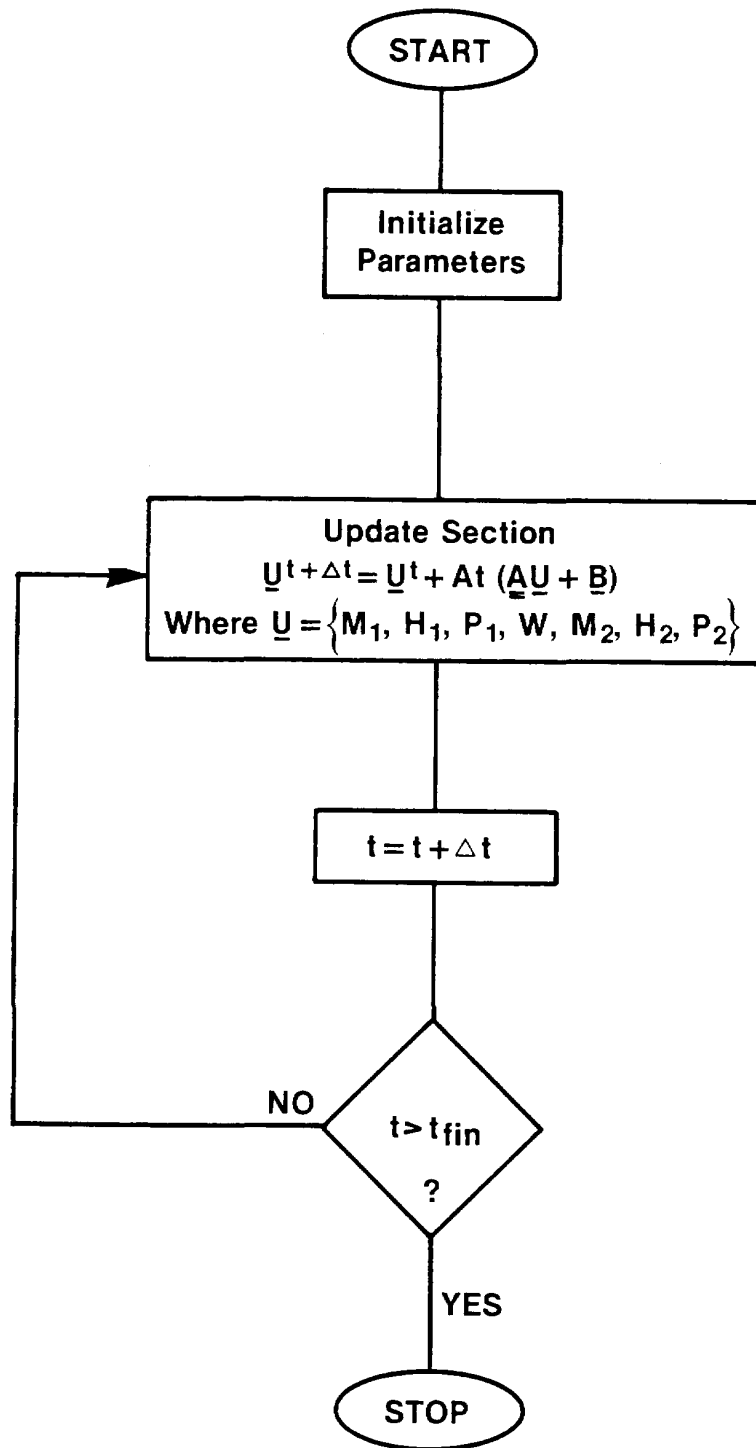


Figure 5.3 Program flow diagram for the rate method.

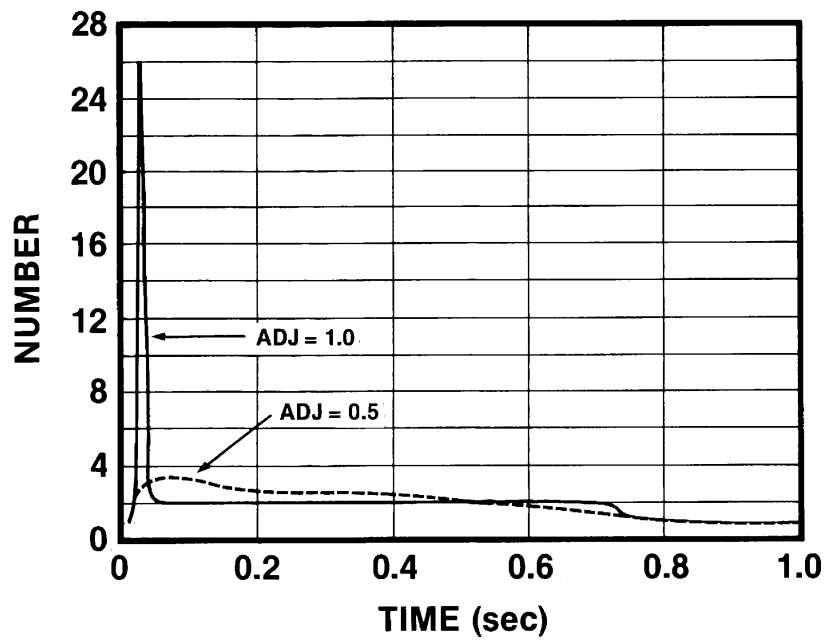


Figure 5.4 Number of iterations per pressure routine call for the normal method with a time step of 0.01 seconds and a pressure error tolerance of 0.001 of full scale (10 mPa).

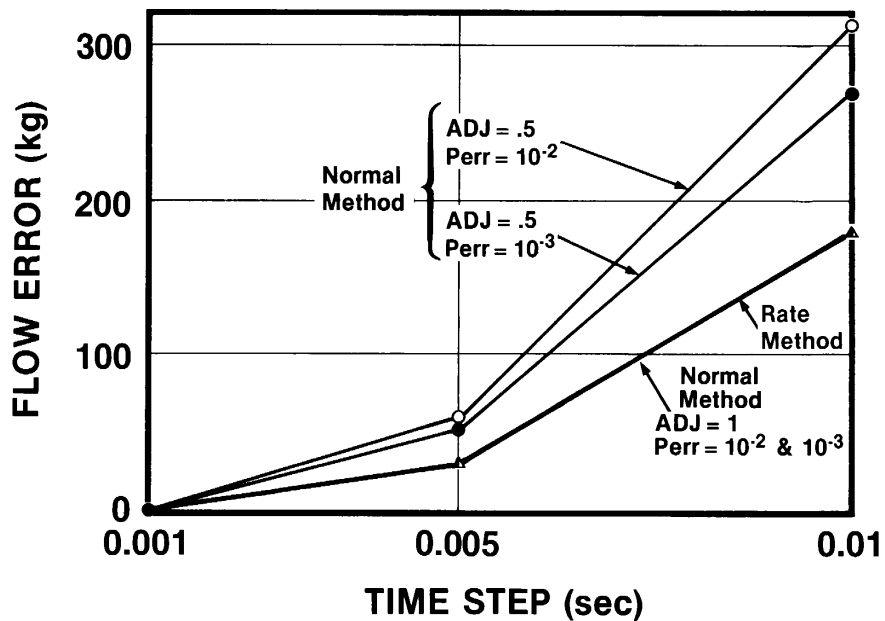


Figure 5.5 Integrated flow error for the rate method and the normal method for various fixed time steps, convergence tolerances and adjustment factors.

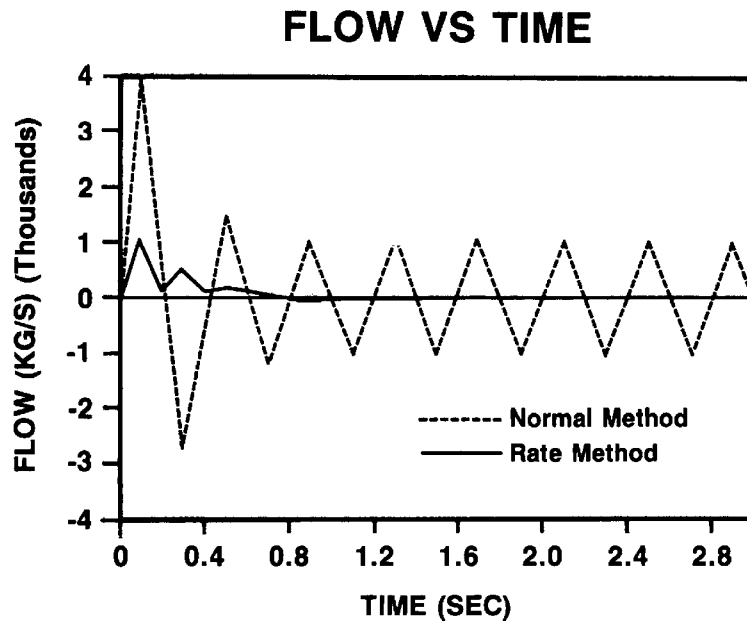


Figure 5.6 Flow vs. time for the implicit forms of the normal and rate method.

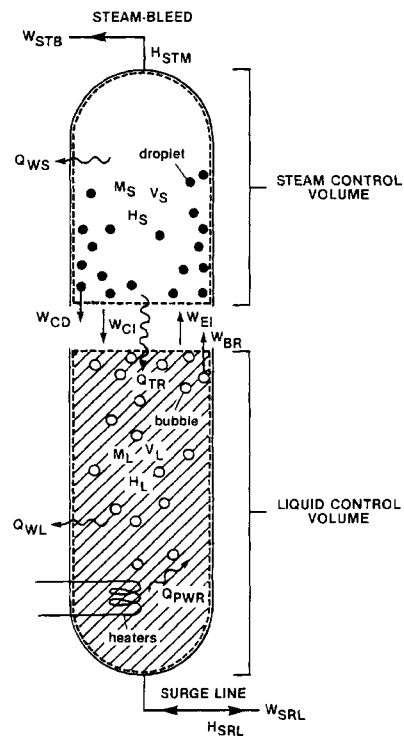


Figure 5.7 Schematic of control volumes in the pressurizer.

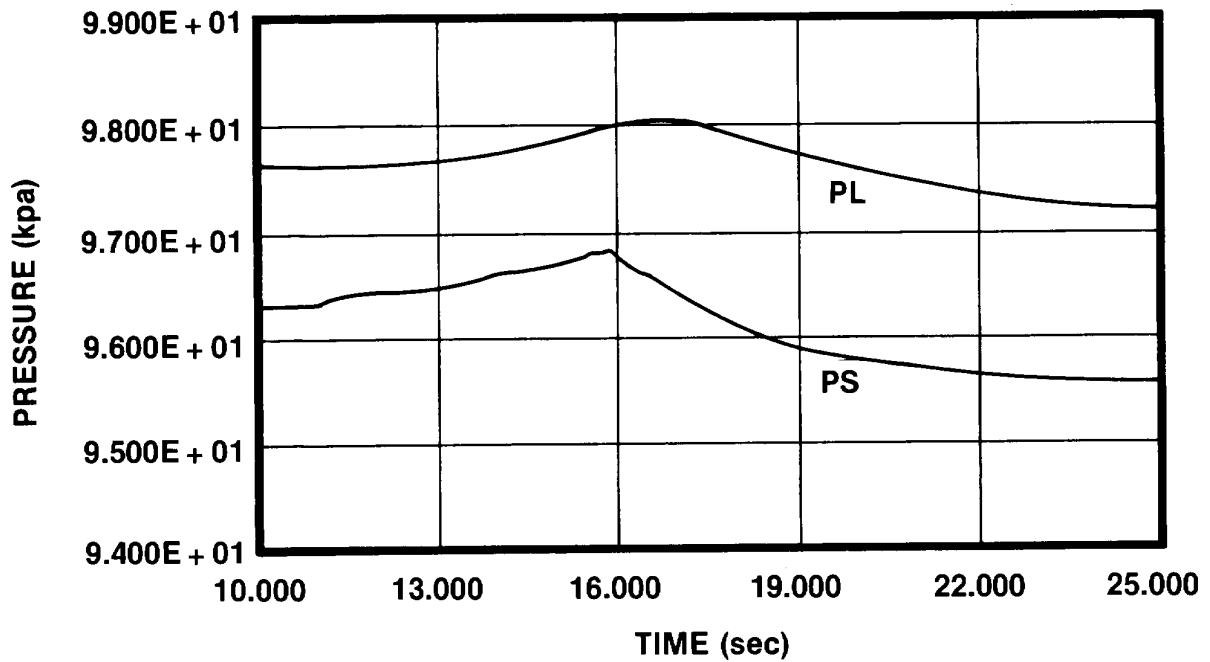


Figure 5.8 Pressurizer's pressure transient for the normal method with error tolerance of 0.2%.

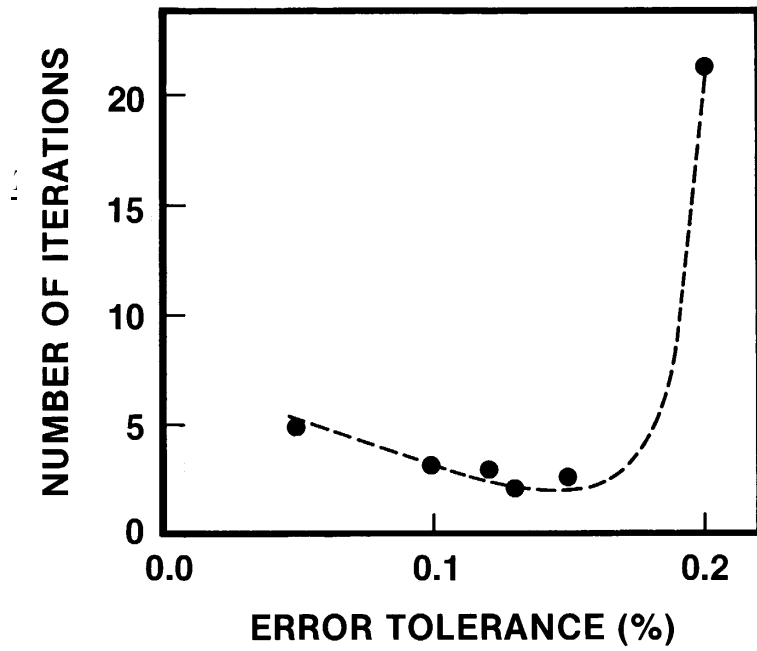


Figure 5.10 Averaged number of iterations per pressure routine call for the normal method in simulating pressurizer problem.